Bandwidth of a 4.7 THz beam multiplexer based on Fourier grating

Gan, Y.; Mirzaei, B.; Silva, J. R.G.; Laauwen, W.; Van Der Tak, F. F.S.; Gao, J. R.

DOI
10.1088/2040-8986/ac62e9

Publication date
2022

Document Version
Final published version

Published in
Journal of Optics (United Kingdom)

Citation (APA)
Gan, Y., Mirzaei, B., Silva, J. R. G., Laauwen, W., Van Der Tak, F. F. S., & Gao, J. R. (2022). Bandwidth of a 4.7 THz beam multiplexer based on Fourier grating. *Journal of Optics (United Kingdom)*, *24*(6), Article 064006. https://doi.org/10.1088/2040-8986/ac62e9

Journal of Optics

PAPER

Bandwidth of a 4.7 THz beam multiplexer based on Fourier grating

To cite this article: Y Gan *et al* 2022 *J. Opt.* **24** 064006

IOP Publishing Journal of Optics
J. Opt. 24 (2022) 064006 (7pp) https://doi.org/10.1088/2040-8986/ac62e9

Bandwidth of a 4.7 THz beam multiplexer based on Fourier grating

Y Gan[1,3,*], B Mirzaei[1,2], J R G Silva[1,3], W Laauwen[1], F F S van der Tak[1,3] and J R Gao[1,2,*]

[1] SRON Netherlands Institute for Space Research, Landleven 12, 9747 AD Groningen and Niels Bohrweg 4, 2333 CA Leiden, The Netherlands
[2] Optics Research Group, Department of Imaging Physics, Delft University of Technology, Lorentzweg 1, 2628 CJ Delft, The Netherlands
[3] Kapteyn Astronomical Institute, University of Groningen, Landleven 12, 9747 AD Groningen, The Netherlands

E-mail: y.n.gan@sron.nl and j.r.gao@sron.nl

Received 17 November 2021, revised 11 March 2022
Accepted for publication 31 March 2022
Published 3 May 2022

Abstract

We present an analysis of the bandwidth of an asymmetric 8-beam Fourier grating as the beam multiplexer for a 4.7 THz local oscillator used in a heterodyne receiver. We take the grating designed for NASA GUSTO balloon observatory as an example to address the bandwidth question although it does not need to operate over a wide frequency range. By illuminating the grating at different frequencies from 4.445 to 5.045 THz, we simulated the changes of its performance in three aspects using COMSOL Multiphysics: diffraction efficiency, power uniformity, and the angular distribution of the output beams. These parameters can affect the coupling efficiency between the output beams of the grating and the beams of a mixer array. The bandwidth of the grating is found to be 230 GHz, corresponding to 4.9% of the operating frequency, which is sufficient for many applications.

Keywords: bandwidths, Fourier grating, heterodyne detection, terahertz, quantum cascade laser

(Some figures may appear in colour only in the online journal)

1. Introduction

Thanks to its very high spectral resolution ($R > 10^6$), the heterodyne technique [1, 2] is widely used for radio astronomical spectroscopy, planetary remote sensing, medical imaging, and contraband detection [3, 4]. In astronomical observations, it is widely used to detect atomic fine structure lines and molecular rotational lines in the terahertz (THz) frequency region from the interstellar medium (ISM). Heterodyne receivers convert a sky signal in THz down to gigahertz frequency by mixing the weak celestial signal with a signal from a local oscillator (LO). In the supra-THz region (>1 THz), quantum cascade lasers (QCLs) [5] provide considerably higher output powers compared to other LO sources based on multipliers [6]. Therefore, the 4.745 THz bands of both the Galactic/ Extragalactic ULDB Spectroscopic Terahertz Observatory (GUSTO) [7] and the Stratospheric Observatory for Infrared Astronomy (SOFIA) [8], aim for detection of [OI] line emission from the Milky Way and nearby galaxies, such as the Magellanic Clouds, by combining a QCL and a Fourier grating to generate LOs for their 8-pixel (GUSTO) and 7-pixel (SOFIA) hot electron bolometer (HEB) mixer arrays. Phase gratings with different techniques have been demonstrated to be applicable as beam multiplexers due to their relatively high efficiency and ability to produce multiple beams with a uniform intensity distribution, including Dammann gratings [9–11], Fourier gratings [12–17], structured surface reflector gratings [18], and two-dimensional phase gratings [19, 20]. Heterodyne array receivers are crucial to enhance observation speed. In order to detect different spectral lines or the Doppler shift of a target line caused by the linear velocity of the ISM beyond our galaxy, a sizable tuning range of LO will

* Authors to whom any correspondence should be addressed.

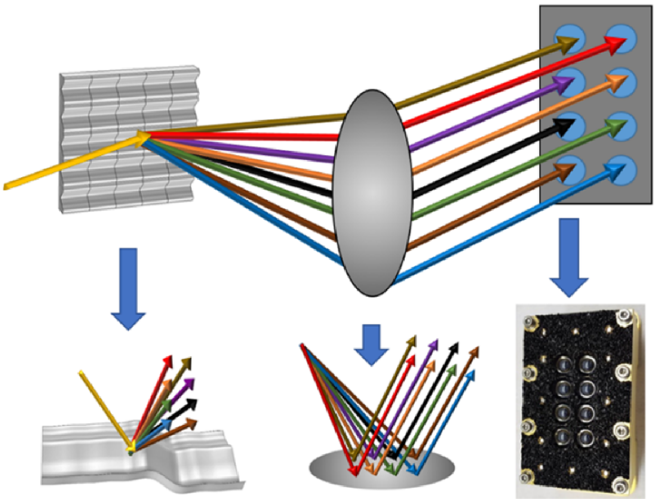

Figure 1. Conceptual diagram of the 4.745 THz 8 beam local oscillator for the GUSTO Observatory. The QCL beam is first diffracted by a reflective phase grating, and is then collimated by a parabolic mirror to form the eight parallel beams. These eight beams are coupled to an 8-pixel quasi-optical HEB mixer array [21].

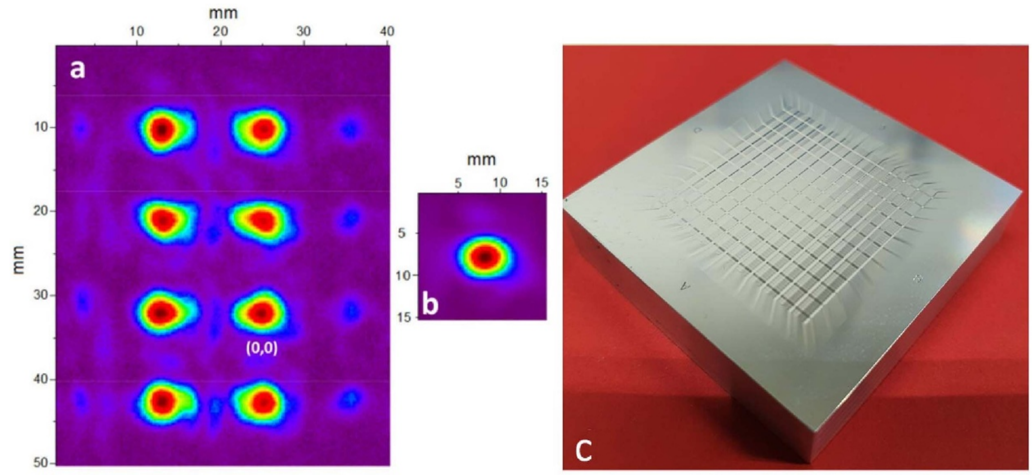

Figure 2. (a) Measured pattern of the image beams of the GUSTO 8-beam Fourier grating [22]. (b) Beam pattern of the input beam to the grating, measured in the same plane as the image beams when the grating is replaced with a flat mirror, to ensure the same air loss for the input and output beams. (c) Optical photo of the tested GUSTO grating.

be necessary since the intermediate frequency (IF) bandwidth of a HEB mixer available in this frequency range is limited (4–10 GHz depending on the HEB). So, an interesting question is how large the bandwidth of a Fourier grating can be. So far, no literature on the phase gratings has addressed this question.

For a Fourier grating in a given receiver system, the change of the source frequency leads to the change of the angular separation and the intensity distribution of the image beams of the grating, causing a loss in the coupling efficiency between the image beams of the grating and the (input) beams of the mixer array. So, the bandwidth of a Fourier grating is characterized by the interplay between the grating and the array. Thus, the bandwidth analysis should take the specific array used into account.

In theory, a Fourier grating can perform well over a wide frequency range by properly changing the input beam incident angle. A grating designed for the frequency f with an incident angle θ_i with respect to the normal works with the same efficiency as long as the product of $f \times \cos\theta_i$ is equal [16]. This provides a very wide band, over which the grating can be used by adjusting the associated optics. For example, the grating we study can operate up to around 9.1 THz if the input beam illuminates the grating with up to 60 degrees with respect to normal. However, since such post-adjustments of the optics in order to adapt for different frequencies are not feasible in practical instrument, in particular, in a space instrument we will consider the cases where the optics is fixed.

Here we analyze the bandwidth of the 8-beam Fourier grating designed for the 4.745 THz array receiver for GUSTO. Figure 1 shows a simplified conceptual diagram of the beams and their propagation in the array receiver. A single QCL beam is first diffracted to eight beams by a reflective Fourier grating, which are collimated by a parabolic mirror, making them parallel to each other. The eight parallel beams are then coupled to the lens-antennas of the mixer array. GUSTO itself does not require a large bandwidth since it aims to detect only [OI] lines mainly from the Milky Way. The GUSTO gratings have been designed and manufactured. One of them has been characterized experimentally and compared to the simulation results. Figure 2 shows the measured beam pattern and a photo of a tested GUSTO grating. The measured results have a good agreement with the simulated results [22], confirming that the simulation by COMSOL Multiphysics is able to predict the performance of the Fourier grating. Therefore, we analyze the bandwidth of the 8-beam Fourier grating also by COMSOL Multiphysics. Some of our earlier analyses have been reported in a conference proceedings [23].

2. Simulated 4.745 THz Fourier grating

A phase grating consists of a periodic structure to diffract a single beam to multi-beams in different directions through phase modulation. According to diffraction theory, the diffracted far field distribution from a grating can be expressed as the Fourier transform of the grating's transmission/reflection function [24]. Gratings using Fourier synthesis technique to achieve continuous phase-only groove shapes are called Fourier gratings [25]. To design a Fourier grating, we expanded the phase modulation function of the grating to Fourier series with a set of Fourier coefficients a_n. Using the Fast Fourier Transform and the Standard multidimensional minimization algorithm in Matlab, we found a set of a_n for a one-dimensional grating with the desired number of beams. A two-dimensional grating is generated by superimposing two 1D profiles orthogonally. In our case, one direction is a 2-beam 1D grating, and the other direction is a 4-beam 1D grating. According to the grating equation $D(\sin\theta_m - \sin\theta_i) = m \cdot \lambda$, the direction of the output beam θ_m in the diffraction order m (integer) is determined by the grating period D, the incident angle with respect to the normal of the grating θ_i and working wavelength λ. An asymmetric grating was designed to accommodate the requirements of the optical system by employing consecutive diffraction orders [22, 26]. In our simulation, for the 4-beam 1D grating, we chose the (−2, −1, 0, +1) diffraction orders, and for the 2-beam 1D grating, we chose the (−1, 0) diffraction orders. The surface topology and specifications (as simulated with COMSOL Multiphysics [27]) of the design are shown in figure 3 and table 1, respectively.

If the incident angle increases, the power variation among the diffracted beams becomes larger [15]. The different unit cell size in two directions is to make the angular distribution in these two directions to be the same. The diffraction efficiency is defined as the ratio of the total diffracted beam power to the power of the incoming beam. The power variation is simulated by COMSOL Multiphysics by importing the surface topology of the grating. We apply the periodic port with periodic boundary condition in the RF module, and extract the S-parameters of the port. The power distribution of the output beams is plotted in figure 4(a), where the X-axis is the mode of the output beam and the Y-axis is the power of the output beam relative to the input beam, expressed as a percentage. We find the largest variation to be 12.5% (between the maximum power and the minimum power). By importing the surface profile of the designed unit cell of the grating and by repeating it in both orthogonal directions, while taking the input as a Gaussian beam, we simulated the far field beam pattern of the grating. The outcome is shown in figure 4(b), where the m and n are the diffraction orders in both directions. From the results in figure 4, we conclude that the grating achieves a good power uniformity among the output beams.

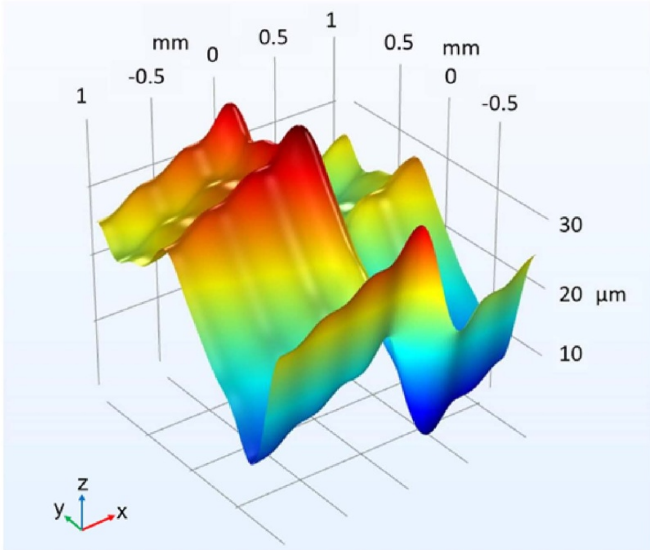

Figure 3. Surface topology of one-unit cell of the grating. The input QCL beam illuminates the grating surface with an incident angle 15° in the *x* direction and 0° in the *y* direction.

Table 1. Grating specifications.

Working frequency	4.745 THz
Material	Aluminum (Aloca QC-10 Mold Alloy)
Angular separation of adjacent beams	∼1.83°
Incident angle	15°
Unit cell size	2.04 × 1.979 mm
Diffraction orders	(−1, 0) (−2, −1, 0, 1)
Diffraction efficiency	70.2%
Uniformity deviation = $(I_{max} - I_{min})/I_{average}$	12.5%

3. Calculation of the grating bandwidth

The 8 beams from the grating are used to pump an 8-pixel HEB mixer array [21]. The power variation among the LO beams can degrade the sensitivity of the mixers in the array since it depends on LO power [17]. We assume that the sensitivity should be within 5% of the optimal value, and we also assume all HEBs in the array require the same LO power. The corresponding LO power variation is estimated to be ∼21%

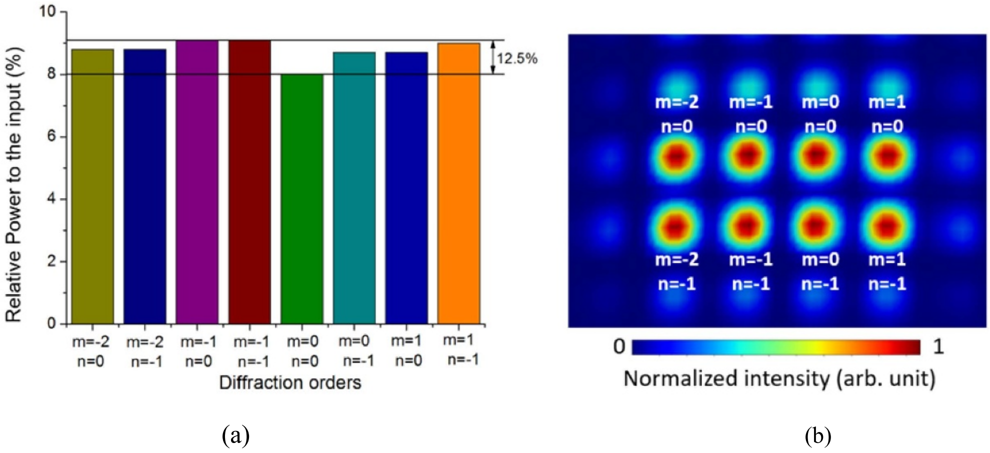

Figure 4. (a) Power distribution of the eight diffracted beams from the grating. The largest variation is 12.5% (between the maximum power and the minimum power). (b) Far field beam pattern of the grating, where *m* and *n* are the diffraction orders in two directions.

Table 2. Diffraction efficiencies η corresponding to different input beam frequencies f from 4.445 THz to 5.045 THz.

f(THz)	4.445	4.545	4.645	4.745	4.845	4.845	5.045
η	70.6%	70.5%	70.4%	70.2%	70.0%	69.7%	69.4%

using the isothermal technique [28, 29][4]. In this paper, we use this criterion to define the bandwidth of the grating, namely, as the frequency range, in which the LO power variation among the array mixers stays below 21%.

The change of the frequency affects the performance of the grating in three aspects; diffraction efficiency, power distribution and angular configuration of the output beams, all influencing the coupling to the mixer array. To analyze these three aspects, we illuminate the grating with a Gaussian beam with a 2.2 mm beam waist at different frequencies from 4.445 to 5.045 THz in COMSOL Multiphysics. The simulation results for the diffraction efficiency are shown in table 2.

Table 2 suggests that the maximal change in diffraction efficiency by varying the frequency is 0.8%, which can be regarded as negligible compared to other two effects (the power distribution and the angular distribution) to be described.

When the grating works at the nominal (or designed) frequency of 4.745 THz, its maximal power variation of the output beams is 12.5% (between the maximum power and the minimum power). When the frequency changes, this number increases since the power distribution among the output beams varies. Figure 5 plots the power distribution of the output beams of the grating operated at different frequencies, where the X-axis is the mode of the output beam and the Y-axis

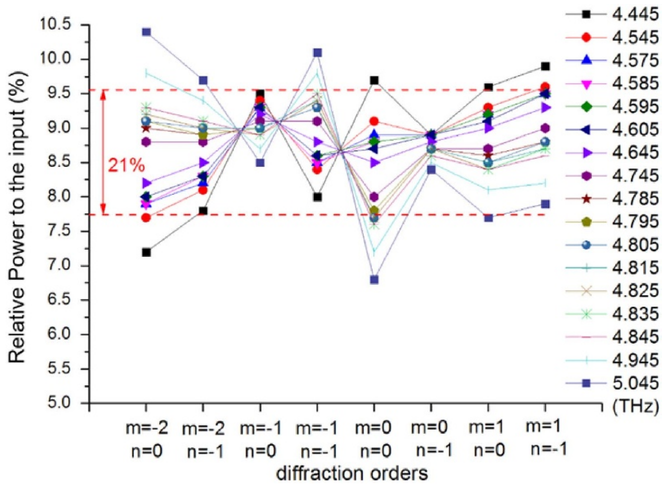

Figure 5. Power distribution of the output beams when the working frequency changes from 4.445 THz to 5.045 THz. Red dashed lines indicate the LO power boundaries, within which the powers of the output beams vary within 21% around their average value.

is the relative power of the output beam to the input beam as a percentage. The red dashed lines indicate the LO power boundaries, within which the power of the output beams varies within 21% around their average value. From figure 5, when the frequency changes between 4.575 and 4.825 THz, the relative powers of all the output beams from the grating vary within 21% around their average value (8.6%). Based on this we derive that the bandwidth of the grating is 250 GHz.

Now we examine the angular distribution of the output beams as a function of the frequency. Since the pixel spacing of the mixer array is fixed, the change in the spacing of the beams can lead to offsets with respect to those of the mixer

[4] The isothermal technique is based on the assumption that an HEB mixer has the same response to LO power and DC power. Thus, we can estimate the absorbed LO power in a mixer from the pumped current–voltage curves. In [29] Khosropanah *et al* measured a set of current–voltage curves of a similar HEB mixer pumped with different LO power operated at 4.3 THz and relevant noise receiver temperatures, from which it was found that when the LO power varies within ~21% the change of HEB receiver noise temperature is not more than 5%.

Table 3. Angular separation of the diffracted beams at the input beam frequency varying from 4.445 to 5.045 THz.

Frequency (THz)	4.445	4.545	4.575	4.585	4.595	4.605	4.645	4.745	4.785
Angular distribution (°)	1.95	1.91	1.90	1.89	1.89	1.88	1.87	1.83	1.82
Offset (mm)	0.43	0.28	0.24	0.22	0.21	0.19	0.14	0	0.05
Frequency (THz)	4.795	4.805	4.815	4.825	4.835	4.845	4.945	5.045	
Angular distribution (°)	1.82	1.81	1.80	1.80	1.80	1.79	1.76	1.72	
Offset (mm)	0.07	0.08	0.09	0.11	0.12	0.13	0.26	0.38	

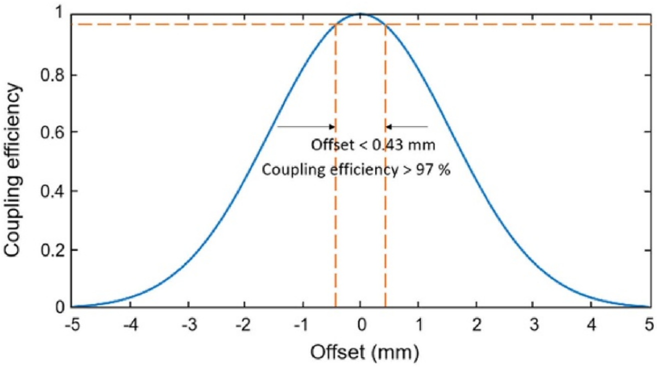

Figure 6. Change of the coupling efficiency between the output beams and the mixer array caused by the spatial offset between them (or misalignment). The orange dashed lines indicate that the coupling efficiency is >97% even with the largest offset 0.43 mm from table 3.

array, which deteriorates the coupling. We calculated the changes of the angular separation by varying the frequency, as shown in table 3. Assuming that the distance between the grating and the mixer array is 200 mm, the offset caused by the different angular separation can also be calculated.

We calculate the coupling efficiency K_{offset} between two Gaussian beams when an offset exists according to the following equations [30]:

$$K_{\text{offset}} = e^{-2\left(\frac{x_0}{\sigma_{\text{off}}}\right)^2}, \quad (1)$$

where x_0 is the offset between the beams and σ_{off} is the offset where the coupling decreases to 1/e, which in our case can be expressed as [30]:

$$\sigma_{\text{off}} = \sqrt{2}\omega, \quad (2)$$

where ω is the beam waist of the Gaussian beam, which is 2.2 mm. Using equations (1) and (2) the coupling efficiency as a function of the offset is plotted in figure 6, from where we found that when the offset between two Gaussian beams is smaller than 0.43 mm, the coupling efficiency between them is larger than 97%.

Combining the coupling efficiency data in this graph and the power distribution in figure 5, we can obtain the power distribution at different frequencies by taking the effect of the angular distribution into consideration. The results are presented in figure 7.

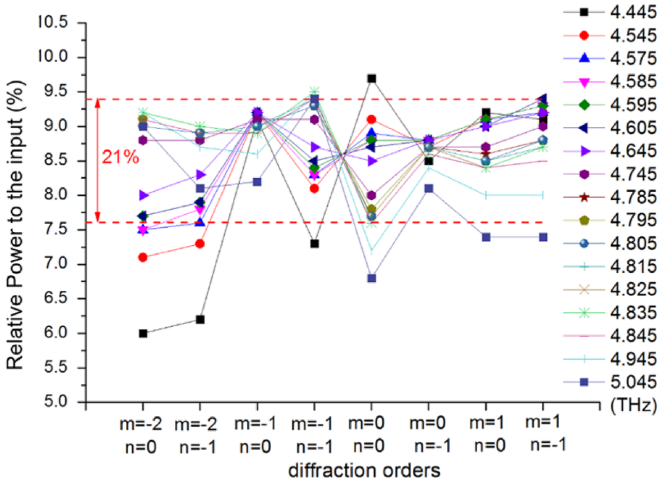

Figure 7. Power distribution of the output beams when the working frequency varies from 4.445 to 5.045 THz, which takes the effect of the angular separation deviation into consideration. Red dashed lines indicate the LO power boundaries, within which the powers of the output beams vary within 21% around their average value.

In figure 7 the red dashed lines indicate the LO power boundaries, within which the powers of the output beams vary within 21%. We find that the coupled powers are within 21% by varying the frequency between 4.595 THz and 4.825 THz. Therefore, after taking the effect of the offset caused by the different angular separation at different frequencies into consideration, the bandwidth of the grating is found to be 230 GHz, which is slightly smaller than the value imposed by the power variation of the output beams (250 GHz).

4. Discussions

The bandwidth of 230 GHz, corresponding to 4.9% of the operating frequency, is a very encouraging result because it can cover a quite reasonable frequency range to detect all the spectral lines. In the case of GUSTO, it could detect not only [OI] line, but also other lines such as water lines nearly if the LO was tunable and had enough large tuning range. As stated earlier, GUSTO aims only one single line. So, GUSTO does not allow to verify our bandwidth prediction experimentally.

In addition, experimental verification of the grating bandwidth needs a sufficiently wideband tunable, high-power THz source around 4.7 THz or multiple THz QCLs to cover a sufficiently wide frequency range, both of which are unfortunately not available to us yet. Therefore, we are not able to measure the bandwidth of the grating experimentally.

Until now, most THz QCLs have a relatively small tuning range, e.g. an order of 10 GHz, by temperature and current. Even with such QCLs, one can build a closely packed array of QCL structures with a small increase of the frequency so that by switching on and off a QCL to cover a large frequency range. One of the examples is the QCL array reported in [2], which covers in total 150 GHz band centered around 4.7 THz. There is potential to realize QCLs with a large tuning range because the gain spectrum of THz QCLs can be engineered by quantum design to be broadband over a range of ∼1 THz. We noticed a record large continuous tuning range of over 330 GHz demonstrated in a double-metal, wire laser configuration THz distributed feedback laser by manipulating the lateral size of the lasing mode via electro-mechanical components [31].

The bandwidth 230 GHz of the grating corresponding to 14 500 km s^{-1} linear velocity is large enough to cover the line frequency shifts of typical galactic (1.6 GHz being equivalent to ∼100 km s^{-1}) and extragalactic (16 GHz to ∼1000 km s^{-1}) objects [1] due to the Doppler effect. The other applications of heterodyne detection, such as the above mentioned planetary remote sensing, medical imaging and contraband detection, also benefit from building heterodyne arrays. Using a QCL with a tunable frequency and a phase grating as the LO could improve the bandwidth of the detector array and thus cover more spectral lines.

5. Conclusions

We numerically evaluated the bandwidth of an asymmetric Fourier grating designed preliminary for an 8-beam LO at 4.745 THz in three aspects; namely diffraction efficiency, power distribution and angular distribution. We found that for the 4.745 THz asymmetric grating, its output beam power variation remains below 21% when the operating frequency changes from 4.595 to 4.825 THz, which gives the frequency bandwidth of 230 GHz and corresponds to about 4.9% of the operating frequency of the grating. The effect is dominated primary by the angular distribution and then by the power distribution, while the diffraction efficiency plays no role since it remains nearly unchanged. Although we focus only at one specific grating, we believe that our approach present here should be applicable for any combinations of a grating based multiple beam LO with a detector array.

Data availability statement

The data that support the findings of this study are available upon reasonable request from the authors.

Acknowledgments

We thank Yuchen Luo for developing the simulation code for the surface topology of a grating, Matvey Finkel and Stephen Yates for their valuable inputs, Matt Underhill (at ASU) for fabricating the grating, and Paul Urbach for his advice on grating modeling. We also thank J. G. bij de Vaate for supporting the PhD activity of Y. G. within the Instrument Science Group at SRON. Y. G. was funded partly by the China Scholarship Council (CSC) and partly by University of Groningen.

ORCID iD

Y Gan https://orcid.org/0000-0002-0132-1426

References

[1] Walker C K 2016 *Terahertz Astronomy* (Boca Raton: CRC Press)

[2] Kloosterman J L, Hayton D J, Ren Y, Kao T Y, Hovenier J N, Gao J R, Klapwijk T M, Hu Q, Walker C K and Reno J L 2013 Hot electron bolometer heterodyne receiver with a 4.7-THz quantum cascade laser as a local oscillator *Appl. Phys. Lett.* **102** 011123

[3] Siegel P H 2002 Terahertz technology *IEEE Trans. Microw. Theory Tech.* **50** 910–28

[4] Siegel P H 2004 Terahertz technology in biology and medicine *2004 IEEE MTT-S Intl. Microwave Symp. Digest* (*Fort Worth, TX, June*) pp 1575–8

[5] Khalatpour A, Reno J L and Hu Q 2019 Phase-locked photonic wire lasers by π coupling *Nat. Photon.* **13** 47

[6] Siles J V, Lin R H, Lee C, Schlecht E, Maestrini A, Bruneau P, Peralta A, Kloosterman J, Kawamura J and Mehdi I Development of high-power multi-pixel LO sources at 1.47 THz and 1.9 THz for astrophysics: present and future *26th Int. Symp. on Space Terahertz Technology (ISSTT 2015)* pp 40–42

[7] Walker C K *et al* 2018 GUSTO: Gal/Xgal U/LDB spectroscopic-stratospheric terahertz observatory *American Astronomical Society Meeting Abstracts* vol 231

[8] Risacher C *et al* 2018 The upGREAT dual frequency heterodyne arrays for SOFIA *J. Astron. Instrum.* **7** 1840014

[9] Dammann H and Görtler K 1971 High-efficiency in-line multiple imaging by means of multiple phase holograms *Opt. Commun.* **3** 312–5

[10] Murphy J A, Withington S and van de Stadt H Dammann gratings for local oscillator beam multiplexing *Multi-Feed Systems for Radio Telescopes. Astronomical Society of the Pacific Conf. Series (Workshop held in Tucson, Arizona, 16–18 May 1994*) vol 75

[11] Murphy J A, O'Sullivan C, Trappe N, Lanigan W, Colgan R and Withington S 1999 Modal analysis of the quasi-optical performance of phase gratings *J. Infrared Millim. Waves* **20** 1469–86

[12] Graf U U and Heyminck S 2001 Fourier gratings as submillimeter beam splitters *IEEE Trans. Antennas Propag.* **49** 542–6

[13] May R, Murphy J A, O'Sullivan C, Gradziel M and Trappe N 2008 Gaussian beam mode analysis of phase gratings *Proc. SPIE* **6893** 68930G

[14] Hurtado N, Graf U U, Adams H, Honingh C E, Jacobs K, Pütz P, Güsten R and Stutzki J 2014 Optics and cryogenics

for the 1.1 THz multi-pixel heterodyne receiver for APEX *Proc. SPIE* **9153** 915327
[15] Mirzaei B, Silva J R G, Luo Y C, Liu X X, Wei L, Hayton D J, Gao J R and Groppi C 2017 Efficiency of multi-beam Fourier phase gratings at 1.4 THz *Opt. Express* **25** 6581–8
[16] Mirzaei B, Silva J R G, Hayton D, Groppi C, Kao T Y, Hu Q, Reno J L and Gao J R 2017 8-beam local oscillator array at 4.7 THz generated by a phase grating and a quantum cascade laser *Opt. Express* **25** 29587–96
[17] Gan Y, Mirzaei B, Silva J R G, Khalatpour A, Hu Q, Groppi C, Siles J V, van der Tak F and Gao J R 2019 81 supra-THz beams generated by a Fourier grating and a quantum cascade laser *Opt. Express* **27** 34192–203
[18] Defrance F, Casaletti M, Sarrazin J, Wiedner M C, Gibson H, Gay G, Lefèvre R and Delorme Y 2016 Structured surface reflector design for oblique incidence beam splitter at 610 GHz *Opt. Express* **24** 20335–45
[19] Graf U U 2018 Enhanced diffraction efficiency of two-dimensional phase gratings *Opt. Express* **26** 32739–42
[20] Ren Y, Xie G A, Zhang Y L, Liu D, Zhou K M, Miao W, Zhang W and Shi S C 2021 Development of terahertz two-dimensional phase gratings for multiple beam generation based on a high-accuracy phase retrieval algorithm *Opt. Express* **29** 17951–61
[21] Silva J R G, Finkel M, Laauwen W M, Westerveld M, More N, Young A, Kulesa C, Walker C, van der Tak F and Gao J R High accuracy pointing for quasi-optical THz mixer arrays *IEEE Trans. Terahertz Sci. Technol.* **12** 53–62
[22] Mirzaei B, Gan Y, Finkel M, Groppi C, Young A, Walker C, Hu Q and Gao J R 2021 4.7 THz asymmetric beam multiplexer for GUSTO *Opt. Express* **29** 24434–45
[23] Gan Y, Mirzaei B, Silva J R G, Laauwen W, van der Tak F F S and Gao J R Bandwidth of a 4.7 THz asymmetric Fourier grating *30th Int. Symp. on Space THz Technology (ISSTT2019)* (*Gothenburg, Sweden*, *15–17 April 2019*) pp 109–12
[24] Goodman J W 1968 *Introduction to Fourier Optics* (New York: McGraw-Hill)
[25] Bliek P, Deleuil R, Breidne M and Maystre D 1981 Microwave verification of a numerical optimization of Fourier gratings *Appl. Phys.* **24** 147–50
[26] Mirzaei B, Gan Y, Silva J R, Finkel M, Yates S, Laauwen W, Young A, Walker C and Gao J R Asymmetric phase grating as 4.7 THz beam multiplexer for GUSTO *30th Int. Symp. on Space THz Technology (ISSTT2019)* (*Gothenburg, Sweden*, *15–17 April 2019*) pp 114–6
[27] 2019 COMSOL multiphysics (available at: www.comsol.com/rf-module)
[28] Ekström H, Karasik S, Kollerg E and Yngvesson K S 1995 Conversion gain and noise of niobium superconducting hot-electron-mixers *IEEE Trans. Microw. Theory Tech.* **43** 938–47
[29] Khosropanah P, Gao J R, Laauwen W M, Hajenius M and Klapwijk T M 2007 Low noise NbN hot electron bolometer mixer at 4.3 THz *Appl. Phys. Lett.* **91** 221111
[30] Goldsmith P F 1998 *Quasioptical Systems: Gaussian Beam Quasioptical Propagation and Applications* (New York: IEEE Press)
[31] Vitiello M S and Tredicucci A 2011 Tunable emission in THz quantum cascade lasers *IEEE Trans. Terahertz Sci. Technol.* **1** 76–84